UNIVERSITY OF CALIFORNIA,
IRVINE

Physiological Ripples on Scalp Electroencephalogram in Healthy Infants

THESIS

submitted in partial satisfaction of the requirements
for the degree of

MASTER OF SCIENCE

in Biomedical Engineering

by

Sara Anis

Dissertation Committee:
Assistant Professor Beth Lopour, Chair
Professor Frithjof Kruggel
Professor Zoran Nenadic

2020

DEDICATION

To

My Family

for their endless love and support

Table of Contents

List of Figures

List of Tables

ACKNOWLEDGEMENTS

To begin, I would like to thank my thesis advisor, Dr. Beth Lopour. This work would not have been possible without her constant encouragement and advice. Her guidance and belief in me and the significance of this work have been instrumental in its completion. Throughout the project, Dr. Lopour has always dedicated time to discuss and resolve all of my problems, and has been a huge support in the writing phase of this work. Dr. Lopour is an exemplary professor and researcher, and I am sincerely grateful to have had the opportunity to work with her and learn from her expertise.

I would also like to express my sincere gratitude to Dr. Frithjof Kruggel and Dr. Zoran Nenadic for serving on my thesis committee. I thank them for their time and invaluable feedback which has helped this work in many ways. I have also had the pleasure of taking classes with both Dr. Kruggel and Dr. Nenadic, and I feel honored to have learned from them.

I would like to thank Dr. Daniel Shrey for providing the data for this project and offering his clinical perspective in this work.

I would also like to thank all the members of our lab, the Lopouratory. A special thanks to Rachel Smith and Derek Hu for their guidance and advice, to Krit Charupanit for his automatic detection algorithm which has been an essential part of this work, and to Kavya RS and Casey Trevino for the discussions and help on my work.

Additionally, I would like to thank all my friends for their unwavering care and support throughout the years. A special thanks to Sarah Rahman for always checking up on my progress and encouraging me throughout.

Finally, words cannot describe how eternally grateful I am for my family. I would like to thank them for helping me pursue my dreams. I thank my parents for the constant encouragement and for their endless love, care, and support. And I thank my sisters, Safa and Sana, for being my best friends and for always keeping me smiling.

ABSTRACT OF THE THESIS

Physiological Ripples on Scalp Electroencephalogram in Healthy Infants

by

Sara Anis

Master of Science in Biomedical Engineering

University of California, Irvine, 2020

Professor Beth Lopour, Chair

High-frequency oscillations (HFOs) are short bursts of power at frequencies > 80 Hz, and they are thought to be significant markers of both cognition and disease in humans and animals. Physiological HFOs have been associated with basic vision and motor, and memory consolidation processes in humans. There is also a significant interest in high-frequency oscillations as a biomarker for epileptogenicity. Pathological HFOs have been associated with many different types of epilepsy and seen in patients of all ages. While studies of epilepsy are mainly associated with pathological HFOs, these studies can also benefit from studying physiological HFOs.

The initial studies of HFOs were conducted using intracranial electroencephalogram (EEG) recordings; however, there is recent evidence that they can also be detected in scalp EEG. While several studies have successfully used scalp EEG to study high-frequency oscillations, they have primarily focused on epilepsy and pathological HFOs. In contrast,

spontaneously occurring physiological HFOs in healthy human subjects using scalp EEG have received little attention thus far. Therefore, the goal of our study is to measure physiological ripples in healthy infants using scalp EEG and obtain robust estimates of their spatiotemporal characteristics.

Here, we report the detection of spontaneously occurring physiological ripples in the long-term scalp EEG of healthy infant subjects. Events were automatically detected in all sixteen subjects and confirmed via visual validation. In total, 11,771 visually validated HFOs were analyzed. We characterized their duration, peak frequency, root-mean-square (RMS) amplitude, spatial distribution, global HFO rate, and variability of global HFO rate across sleep stages and over time. We found that HFO rate was highest in frontal and temporal channels, and it was highest in the lightest stage of non-REM sleep (N1) across all subjects. Based on 10-minute segments of EEG, the measurements of rate varied over time, with the highest variance in stage N1. We found no relationship between subject age and global HFO rate.

This work represents the most comprehensive analysis of scalp physiological ripples thus far, drawing from almost 180 hours of non-REM sleep EEG. The results contribute to our understanding of the visibility and characteristics of physiological ripples on the scalp and their relationship to the stages of sleep, as well as providing a valuable baseline for studies of pathological ripples associated with epilepsy.

1. INTRODUCTION

1.1 High-Frequency Oscillations are Markers of Cognition

High-frequency oscillations (HFOs) are short bursts of power at frequencies > 80 Hz, and they are thought to be significant markers of both cognition and disease in humans and animals (Buzsáki & Silva, 2012). They are empirically defined as events consisting of four or more oscillations that stand out from background activity in the electroencephalogram (EEG). These events are called ripples when their peak frequency lies in the 80-250 Hz band, and they are called fast ripples when present in the 250-500 Hz band. High-frequency oscillations occurring due to normal physiological processes in the brain are termed "physiological HFOs," as opposed to those associated with diseases such as epilepsy, which we will refer to as "pathological HFOs."

In animals, spontaneous HFOs have been associated with sleep, memory, anesthesia, and sensory stimuli. HFOs of 400-600 Hz of interneurons in the neocortex of rats were observed during sleep spindles, and they were suggested to play a role in the discharge process of pyramidal cell populations (Kandel & Buzsáki, 1997). Some have also been linked to memory. Ripples of 200 Hz observed in the hippocampal-entorhinal output pathway of freely behaving rats suggested their physiological contribution to synaptic modifications in the memory consolidation process (Chrobak & Buzsáki, 1996). Ripples of 80-200 Hz observed in the neocortex of cats under anesthesia and chronic experimental conditions were suggested to play a role in plasticity processes (Grenier et al., 2001). HFOs have also been recorded in response to a stimulus. HFOs greater than 200 Hz were observed in the rat somatosensory cortex in response to a vibrissa stimulation and

contribute to explaining the functional roles of these oscillations in physiological processes (Jones et al., 2000).

In humans, high-frequency oscillations have been associated with basic vision and motor processes. Nagasawa et al., 2012 observed spontaneously occurring and visually driven HFOs (> 80 Hz) in epileptic patients emerging from the occipital cortex. Spontaneous HFOs were observed to be spatially sparse and focal, while visually driven HFOs were found to involve larger areas of cortex. Task-based high-frequency oscillations have also been observed during motor imagery and motor tasks in humans. Smith et al., 2014 observed a significant power increase in high-frequency activity (70-150 Hz) during a motor imagery task using non-invasive recordings in healthy subjects. Other studies have observed HFOs in the human primary motor cortex of epileptic patients in relation to upper extremity movements (Wang et al., 2017) and walking (McCrimmon et al., 2018). A cascade of high-frequency activity has also been observed in language processing and reading tasks through intracranial recordings (Lachaux et al., 2012). There is also evidence that physiological HFOs may occur broadly throughout the brain, with one recent study establishing region-specific normative values for physiological HFOs based on invasive recordings from non-lesional tissue in patients with epilepsy (Frauscher et al., 2018).

Task-based high-frequency oscillations have also been associated with memory consolidation processes in humans. The first study to report HFOs in humans during a cognitive task was presented by Axmacher et al., 2008. They studied intracranial recordings from the rhinal cortex and hippocampus contralateral to SOZ in epileptic patients. Ripples were found in both the rhinal cortex and hippocampus, and a significant correlation was found between the number of rhinal ripples and memory consolidation.

Another study found intracranially recorded HFOs (50-500 Hz) in epileptic patients during memory encoding and recall processes in response to a presentation of images (Kucewicz et al., 2014). HFOs were observed in the primary visual, limbic and cortical regions associated with visual processing flow, and they were localized to the amygdala, hippocampus, and specific neocortical areas, suggesting HFO activity is linked with memory processing. The relationship between ripples and memory consolidation was also observed in Zhang et al., 2018, where they measured replay in intracranial recordings in human epileptic patients and found that replay is related to hippocampal ripples.

1.2 High-Frequency Oscillations are Markers of Epilepsy

There is also a significant interest in HFOs as a biomarker for epileptogenicity (Zijlmans et al., 2012). Epilepsy is one the most common neurological disorders, affecting approximately 1% of the population or 70 million people worldwide (Murin et al., 2018). It consists of abnormal neural activity causing recurrent, unprovoked epileptic seizures, with a range of symptoms. In focal epilepsy, the limited area in the brain that is necessary and sufficient for seizure generation is known as the epileptogenic zone (EZ). The EZ is difficult to map, hence in clinical practice, the EZ is approximated by the seizure onset zone (SOZ), a region where ictal (during seizure) changes in EEG are first seen. While antiepileptic medication helps control these seizures in about 60-70% of patients, it is ineffective in others (Murin et al., 2018). Resective surgery of areas generating these seizures is an alternative option. Recent trials have shown that long-term seizure freedom can be achieved in approximately two thirds of the patients undergoing resective surgery (Murin et al., 2018).

Pathological HFOs have been associated with many different types of epilepsy and seen in patients of all ages. HFOs have been intracranially recorded in the entorhinal cortex and hippocampus of epileptic patients (Bragin et al., 1999; Staba et al., 2002). They have also been shown to be specific in identifying epilepsy in young children (Wu et al., 2008). Moreover, it has been suggested that they are more specific and accurate than epileptic spikes in identifying the SOZ when comparing rates inside and outside the SOZ (Melani et al., 2013; Jacobs et al., 2010; Andrade-Valenca et al., 2011), and more tightly linked to seizures than epileptic spikes when comparing rates before and after seizures (Zijlmans et al., 2009). HFOs were also found to give more information on epileptogenicity than spikes in childhood epilepsy (Kramer et al., 2019) and idiopathic partial epilepsy (Kobayashi et al., 2011). They have also been linked to processes in the generation of myoclonic seizures (Kobayashi et al., 2018). Findings of fast ripples only in epileptic patients as compared to controls (Bernardo et al., 2018), and only near epileptogenic lesions in epileptic patients (Bragin et al., 1999; Staba et al., 2004), suggest that HFOs can serve as a powerful biomarker for localization of epileptic regions, providing clinical significance for surgical treatments.

While studies of epilepsy are mainly associated with pathological HFOs, these studies can also benefit from studying physiological HFOs. One study found that HFOs were not statistically better biomarkers than epileptic spikes, with one contributing factor being the presence of physiological HFOs which weakened their results (Roehri et al., 2018). While there have been efforts to differentiate physiological and pathological HFOs in terms of frequency, duration, amplitude (Matsumoto et al., 2013; Cimbalnik et al., 2018), and sleep stage (von Ellenrieder et al., 2017), it remains a very challenging task since

characteristics of the two overlap. Thus, studying HFO activity in healthy subjects will help us gain a better understanding about the characteristics of physiological HFOs and contribute to improved clinical applications.

1.3 High-Frequency Oscillations can be Measured with Scalp EEG

While the initial studies of HFOs were conducted using intracranial EEG recordings, there is recent evidence that they can also be detected in scalp EEG. Scalp EEG is a non-invasive electrophysiological recording technique which consists of electrodes placed according to the 10/20 international system (Jasper, 1958). The system allows for a standardized procedure for electrode placement, and the 10-20 rule (**Figure 1)** ensures comparably equal spacing between electrodes. Electrodes placed over the right brain hemisphere are even numbered, while those placed over the left hemisphere are odd numbered. The distribution of electrodes covers the prefrontal (Fp), frontal (F), parietal (P), central (C), and occipital (O) regions, with midline channels labeled as Fz, Cz, and Pz **(Figure 1)**.

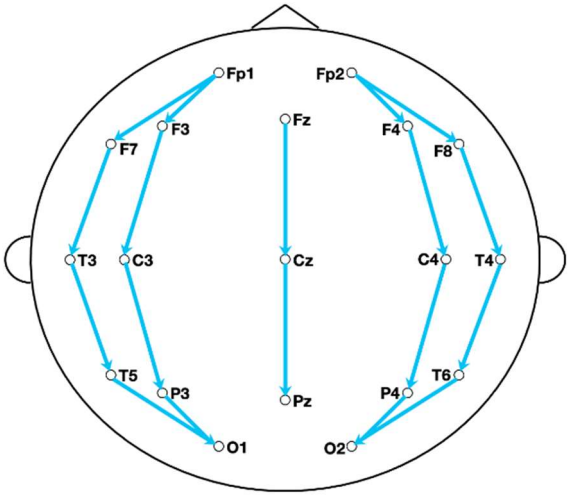

Figure 1. Scalp EEG electrode placement with a longitudinal bipolar montage.

Scalp EEG is highly susceptible to artifacts, such as DC shifts, muscle artifacts, electrode artifacts, ocular artifacts, and cardiac artifacts (St. Louis et al., 2016). Different re-referencing schemes can be employed in analysis of EEG (Polo et al., 2018). The longitudinal bipolar montage consists of referencing pairs of electrodes across the anterior-posterior axis of electrodes, forming a "double banana" across the scalp (**Figure 1**). This montage limits the effect of artifacts by canceling all signals that are common to adjacent electrodes, leaving only highly localized activity.

Scalp EEG serves as a very promising interface for HFO detection. It has been shown that high-frequency oscillations observed on scalp EEG can be produced by small cortical generators, thus indicating that scalp and intracranial recordings can reflect the same cortical generators (Zelmann et al., 2013; von Ellenrieder et al., 2014). Another study also found that high-frequency activity from scalp EEG during a motor imagery task was spatially co-localized with BOLD (blood-oxygen-level-dependent) fMRI data, suggesting that scalp EEG can provide an accurate spatial estimation of local high-frequency activity (Smith et al., 2014). Specifically, in infants, the skull is thinner than in adults (Li et al., 2015), and thus it may be easier to detect HFOs in this population through noninvasive methods.

1.4 Physiological HFOs Measured with Scalp EEG

While several studies have successfully used scalp EEG to study high-frequency oscillations, they have primarily focused on epilepsy and pathological HFOs (Wu et al., 2008; Andrade-Valenca et al., 2011; Melani et al., 2013; Bernardo et al., 2018; Kobayashi et al., 2018; Kramer et al., 2019). Studies on physiological HFOs have mostly relied on

intracranial EEG using subjects with epilepsy (Axmacher et al., 2008; Nagasawa et al., 2012; Kucewicz et al., 2014; Frauscher et al., 2018; Zhang et al., 2018).

In contrast, spontaneously occurring physiological HFOs in healthy human subjects using scalp EEG have received little attention thus far. There has only been one study of spontaneously occurring physiological ripples in scalp EEG (Mooij et al., 2017). They studied ripples during day-time sleep EEG that were free of epileptiform spikes. Their subject cohort consisted of 23 children between the ages of 11 months to 14 years, most of which were subjected to partial sleep deprivation. Subjects were categorized into four categories after a follow-up by a pediatric neurologist: 1. no epilepsy or other brain disorder, 2. no epilepsy, but presence of another brain disorder, 3. benign-course epilepsy, and 4. other types of epilepsy. Ripples were visually marked by viewing EEG in both bipolar and common average montage, and artifactual segments were not included in the analysis. For each subject, the ripple rate calculation was done over the 10-min period which exhibited the highest number of ripples, and spatial distribution results were calculated as a summation of ripple events across all subjects. Characteristic values of frequency, duration, and RMS amplitude of all ripple events were also reported. Subsequently, the relationship between the ripples and sleep phenomena were investigated (Mooij et al., 2018). One third of the ripples co-occurred with sleep-specific transients, especially vertex waves. Also, they found that ripple rates during N1 sleep (light sleep) were higher than N2 and N3 sleep. These findings were significant, as this was the first demonstration that spontaneously occurring physiological HFOs could be measured using scalp EEG.

However, there are a few limitations that can be noted in these studies. The inclusion of both healthy and diseased subjects in their analysis does not allow for

delineation of results for healthy subjects. Thus, a completely healthy cohort has not previously been studied. Also, while the limited amount of data used may be ascribed to visual detection as it is a time consuming process (Spring et al., 2018), their work could have benefitted from including a larger amount of data in order to assess the robustness of the results over time. Additionally, sleep deprivation could have influenced their results as a notable increase in slow-wave activity in the hours post partial sleep deprivation has been reported (Plante et al., 2016).

Therefore, the goal of our study is to measure physiological ripples in healthy infants using scalp EEG and obtain robust estimates of their spatiotemporal characteristics. Our study analyzes long, overnight recordings of non-rapid eye movement (REM) scalp EEG data from healthy infants (<1 year old). We detected HFOs and characterized their duration, peak frequency, root-mean-square (RMS) amplitude, spatial distribution, global HFO rate, and variability of global HFO rate across sleep stages and over time. The recruitment of a cohort consisting only of healthy subjects and our analysis of multiple hours of sleep EEG will provide a comprehensive picture of scalp physiological ripples. This work will contribute to our knowledge of high-frequency activity during cognition and provide baseline measurements that can aid studies of pathological ripples associated with epilepsy.

2. METHODS

2.1 Subjects

This prospective study was approved by the Institutional Review Board of the Children's Hospital of Orange County (CHOC). Data were collected at CHOC as part of a larger study of infantile spasms (IS), or West syndrome, which is a form of epileptic encephalopathy (Pellock et al., 2010). Subjects were between 0-3 years of age and were undergoing inpatient EEG monitoring for suspicion of epileptic spasms. Because we aimed to study physiological HFOs, as opposed to pathological HFOs associated with epilepsy, we selected for analysis all subjects that did not exhibit epileptic spasms during monitoring. These subjects were recruited between June 2017 and January 2019. Further inclusion criteria included a normal vineland developmental score (Sparrow et al., 2016) and normal MRI. Subjects were excluded if any of the following were noted: seizures were observed, subject was on medication at any point in the study, subject had other medical diagnoses, technical error occurred during research recording, or initial results were suspicious for spasms. These exclusion criteria were applied to ensure the cohort consisted only of healthy infants.

2.2 EEG Data Collection

Continuous, overnight video EEG was recorded for each subject, with recordings starting after consent was obtained and stopping when it was confirmed that the subject did not exhibit epileptic spams. EEG data were acquired with 19 electrodes placed according to the international 10-20 system. The sampling rate was 5 kHz, using a Neurofax EEG-1200

acquisition system with JE-120A amplifier fitted with a QI-124A dual data stream recording unit (Nihon Kohden, Tokyo, Japan). Recordings were visually sleep staged by a registered polysomnographic technologist (Cristal Garner, REEGT, RPSGT) in accordance with the American Academy of Sleep Medicine (AASM) guidelines. We extracted the non-REM portions of sleep (stages N1, N2, N3) for our analysis, as it was previously reported that physiological HFOs occur more frequently during these stages and their occurrence may be related to transient sleep-specific waveforms (Grenier et al., 2001; Zhang et al., 2018; Staba et al., 2004). Also, many EEG artifacts are reduced or subside during sleep.

2.3 HFO Detection

The HFO detection process consisted of data preprocessing, automated HFO and artifact detection, and visual validation of candidate events (**Figure 2)**. While visual detection is the gold standard for HFO detection, the process is very time consuming and suffers from low interrater reliability (Spring et al., 2018). Numerous automated HFO detection methods have been proposed and developed, achieving high sensitivity and specificity (Staba et al., 2002; von Ellenrieder et al., 2012; Jrad et al., 2017). However, expert review of detected events is advised to minimize false positives, especially when analyzing artifact-prone scalp EEG. Thus, we implemented a combination of automated detection, automated artifact rejection, and visual validation to identify true positive HFOs.

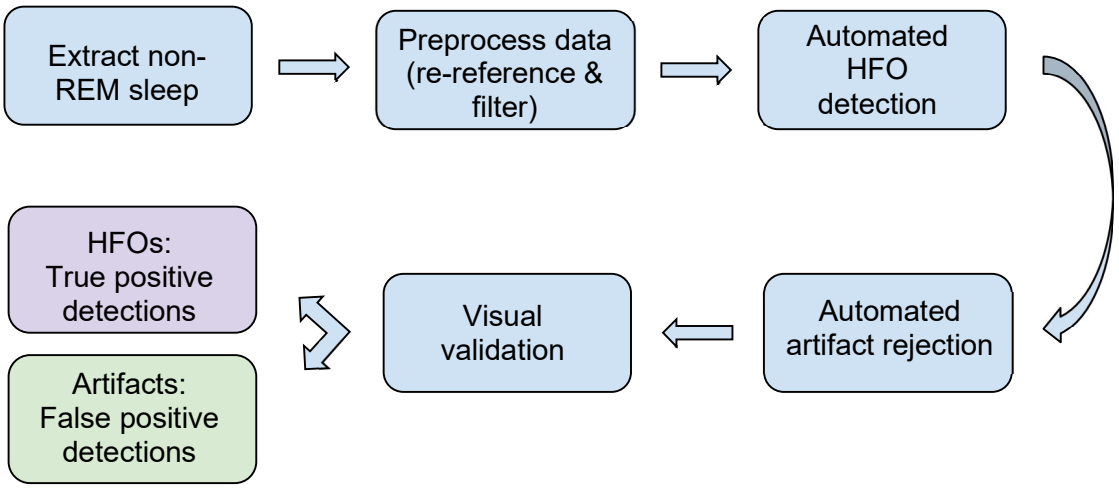

Figure 2. Flowchart of HFO detection process. Segments of non-REM sleep were extracted and preprocessed. Automatic HFO detection was employed, followed by automated artifact rejection. Resulting candidate events were visually validated to identify HFOs.

2.3.1 Data Processing

All analysis was completed using custom written code in MATLAB (version R2018b, The MathWorks Inc., USA.). We extracted all non-REM sleep EEG data for subjects based on visual sleep staging information. For all subjects, each continuous segment of non-REM sleep data was placed in a separate file for HFO analysis. Median segment duration was 29.53 minutes (IQR 13.44-50.48 minutes). All EEG was re-referenced using the longitudinal bipolar montage and filtered in the ripple band (80–250 Hz) using a finite impulse response filter (Zijlmans et al., 2012). Signals were filtered forward and backward to ensure zero-phase distortion.

2.3.2 Automatic Detection

Automated HFO detection was accomplished using a previously validated automated detector that has been applied to both intracranial EEG (Charupanit & Lopour, 2017) and

scalp EEG (Charupanit et al., 2018). Briefly, this detector requires optimization of a single parameter, α, which is used to identify events in the ripple band that have three oscillations (six consecutive peaks in filtered, rectified data) above a threshold. The threshold is calculated through an iterative process that estimates the amplitude distribution of the background activity. In this study, the threshold was calculated for every continuous 5-second segment of data. Windowing the data in 5-second intervals for detection improved rejection of muscle noise, as the detector automatically chose a higher threshold for periods containing high amplitude muscle activity. For each subject, a single α value was used for all channels and all sleep data, with values ranging from 0.001 to 0.005 (see Section 2.3.4 for more details).

2.3.3 Automated Artifact Rejection

We applied five post-processing steps to the candidate events resulting from automatic detection, in order to reduce false positive detections caused by artifacts. These steps applied additional criteria for the maximum duration, maximum amplitude, maximum difference, line length, and number of zero crossings. Methods were applied either to the raw (bipolar re-referenced) or ripple (band-pass filtered) data. The threshold for maximum duration was determined based on past literature; the threshold optimization process for the other four methods can be found in Section 2.3.4.

2.3.3.1 Maximum Duration

HFOs typically have a duration of 40-100 ms (von Ellenrieder et al., 2012). Longer events tend to be detected due to higher amplitude background activity associated

with muscle artifact. Thus, candidate events with duration > 200 ms in the ripple data were excluded.

2.3.3.2 Maximum Amplitude

Median RMS amplitude values of scalp HFOs have been observed to be between 0.95-5.24 μV (Zelmann et al., 2013; Mooij et al., 2017), with typical examples exhibiting amplitudes of roughly 5 μV (Andrade-Valenca et al., 2011; Zelmann et al., 2013; Mooij et al., 2017). Also, candidate events of non-neural origin, e.g., due to filtering of sharp spikes (Zijlmans et al., 2012), were observed to have extremely high amplitude in our parameter optimization process. Thus, candidate events with maximum amplitude > 20 μV in the ripple data were excluded. Maximum amplitude was calculated based on the duration of the candidate event only.

2.3.3.3 Maximum Difference

DC shifts, sharp spikes, and electrode pop artifacts in the raw data are other common artifacts. When filtered in the ripple band, these waveforms may look very similar to a true high-frequency oscillation (Zijlmans et al., 2012). Thus, candidate events with maximum difference > 50 μV between successive data points in the raw data (indicative of a high amplitude spike or shift) were excluded. Maximum difference was calculated based on a larger window of data including the duration of the candidate event +/- 150 ms.

2.3.3.4 Line Length

Muscle activity in the raw data is a common source of EEG artifacts (Zijlmans et al., 2012). When filtered in the ripple band, these artifacts may look similar to a true high-frequency oscillation. However, they differ from true HFOs in that they often have a high amplitude in the raw data and a longer duration. Thus, candidate events with line length > 2000 (units: $\sqrt{\mu V^2 + s^2}$) in the raw data were excluded. Line length was calculated as the sum of distances between successive points in time based on a larger window of data including the duration of the candidate event +/- 150 ms.

2.3.3.5 Number of Zero Crossings

Segments of raw data that excessively cross the zero line are considered artifactual and can be a source of false positive HFO detections (Liu et al., 2016). Thus, candidate events with > 20 zero crossings in the raw data were excluded. Number of zero crossings was calculated on the duration of the candidate event only.

2.3.4 Parameter Optimization

For each subject, we randomly selected one 10-minute segment of sleep data. The α values for each subject and the cutoff thresholds for the four artifact rejection methods were empirically determined based on visual analysis of these segments. Optimal alpha values differed for each subject (listed in **Table 1**), while optimal cutoff values for the four artifact rejection methods were consistent across subjects.

2.3.5 Visual Validation

The five post-processing steps reduced the number of false positive detections, but the thresholds were chosen to remove only the most egregious artifacts. Using stricter thresholds risked rejecting some HFOs. Therefore, in order to maximize the specificity of our detection, we visually validated each event remaining after automated detection and automated artifact rejection. Visual validation was performed using a custom MATLAB graphical user interface with scrolling functionality to change the time period displayed; both the broadband data (low cutoff, high pass filtered data) and ripple data surrounding each candidate event were displayed (**Figure 3**).

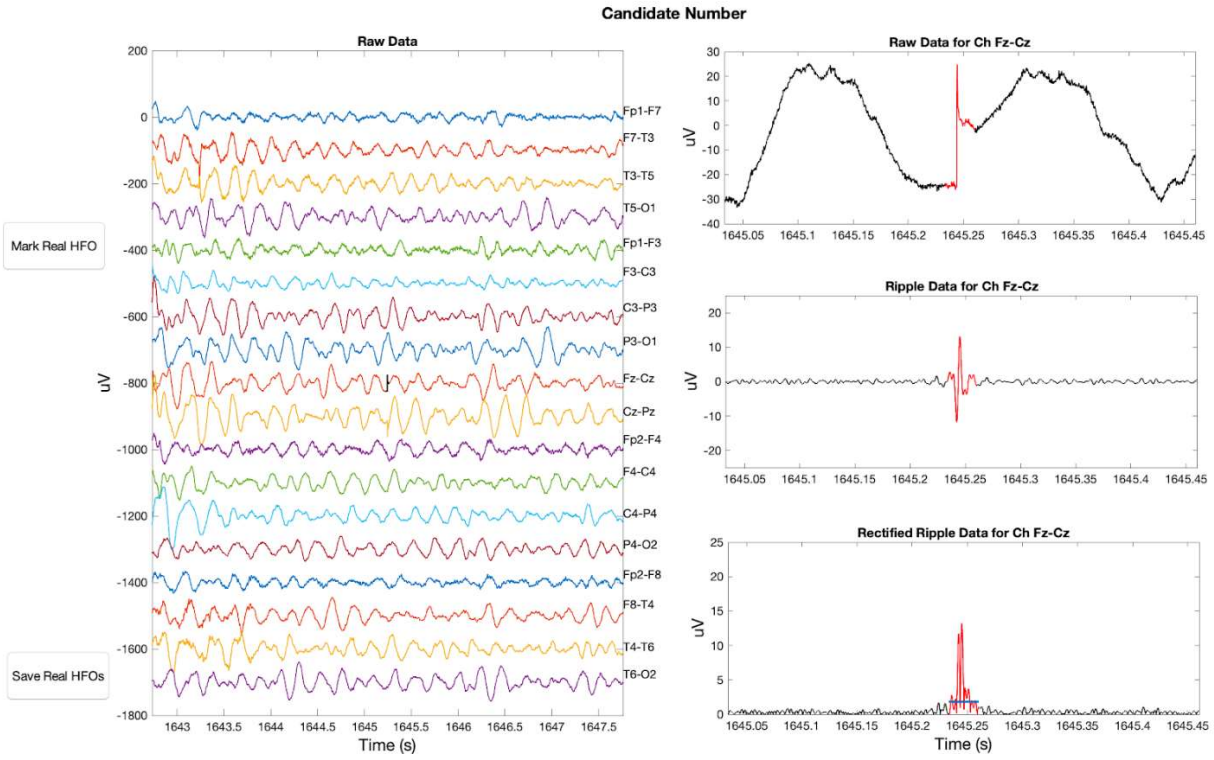

Figure 3. Custom interface for visual validation process. In the left panel, 5 seconds of broadband data is displayed for all channels. The right panel shows 400 ms of broadband data (top), ripple band filtered data (middle), and rectified ripple data (bottom) surrounding each candidate event in its specific channel. The detection threshold for the event is displayed as a blue horizontal line on the rectified ripple data. In this particular example, a detection resulting from a DC shift artifact is shown.

Two criteria were used to exclude events as false positive detections: (1) if the raw data contained a DC shift/spike with no visible oscillations, or (2) if there was muscle activity in the channel containing the candidate event or its adjacent channels. Characteristics such as minimum event duration and amplitude (whether or not the oscillation stands out from background activity) were inherent to the design of the automated detector used in this study, and thus were not explicitly included in the visual criteria.

2.4 Analysis

We characterized the visually validated HFOs by measuring their duration, peak frequency, and root-mean-square (RMS) amplitude. We also calculated the spatial distribution and global HFO rate for all non-REM sleep and the individual sleep stages, as well as the temporal variability of global HFO rate for each sleep stage. Duration was defined as the end time minus start time of the event, as indicated by the automated detector. Peak frequency was calculated using the Fourier Transform, with zero-padding to increase the frequency resolution to 1 Hz. Root-mean-square amplitude was calculated for each event in the ripple band as the square root of the mean of the squared data.

To measure the spatial distribution of the HFOs, we calculated the average HFO rate for each channel and then averaged across subjects. For all non-REM sleep, this was the total number of HFOs per minute for each channel (thus, normalized to each individual subject's total non-REM sleep time). For individual sleep stages, this was the total number of HFOs per minute per sleep stage for each channel (thus, normalized to each individual subject's sleep time in that specific sleep stage). For each individual subject, global HFO

rate for all non-REM sleep was calculated as the total number of HFOs summed across all channels divided by total non-REM sleep time for that subject. For each individual subject, global HFO rate for individual sleep stages was calculated as the total number of HFOs per sleep stage summed across all channels divided by total time in the respective sleep stage for that subject. To determine the variability of global HFO rate over time for each sleep stage, global HFO rate per 10-minute intervals for individual sleep stages was calculated for each subject.

We also performed the same analysis on artifacts that were rejected in the visual validation step to determine the characteristics of the rejected events. A Wilcoxon rank-sum test was used to compare the duration, peak frequency, and RMS amplitude between HFOs and artifacts within individual subjects (Mann & Whitney, 1947). We also used Friedman's two-way analysis of variance by ranks test (Friedman's ANOVA) to determine if there was a difference in ripple rates between sleep stages across all subjects. Wilcoxon's signed-rank test was used for post hoc testing (Wilcoxon, 1945). To determine the difference in ripple rates between sleep stages for individual subjects, the Wilcoxon rank-sum test was used.

3. RESULTS

3.1 Subjects

Based on the inclusion and exclusion criteria, sixteen normal subjects were included in our final cohort (4 males/12 females, median age 6.16 months, IQR 2.63-8.15 months). Median non-REM sleep EEG duration was 10.40 hours (IQR 9.03-12.63 hours), for a total of 179.16 hours of non-REM sleep data. Median N1 sleep data duration was 4.14 hours (IQR 2.23-4.70 hours), for a total of 60.83 hours of N1 sleep data. Median N2 sleep data duration was 5.32 hours (IQR 4.32-6.76 hours), for a total of 96.49 hours of N2 sleep data. Median N3 sleep data duration was 1.42 hours (IQR 0.75-1.97 hours), for a total of 21.85 hours of N3 sleep data. Subject demographics and duration of EEG data are shown in **Table 1**.

Table 1. Cohort demographics.

Subject	Sex/Age (months)	Total non-REM Sleep Data (hrs)	Detection threshold (α)	Global HFO rate per min
1	M / 2.07	7.88	0.005	2.22
2	M / 7.72	9.96	0.001	1.59
3	F / 8.57	10.48	0.001	1.18
9	F / 4.01	9.41	0.0025	1.67
12	F / 9.33	12.42	0.005	2.20
18	F / 7.42	9.82	0.005	1.11
21	F / 6.96	21.48	0.0025	1.13
22	M / 5.98	12.84	0.0025	1.29

24	F / 3.78	11.71	0.0025	1.14
28	M / 6.34	10.47	0.001	1.05
29	F / 2.56	8.41	0.0025	0.41
30	F / 2.69	10.33	0.0025	0.63
32	F / 11.27	7.42	0.001	0.66
41	F / 2.2	12.89	0.001	0.27
42	F / 11.14	8.66	0.0025	0.70
44	F / 1.97	14.99	0.0025	0.45

3.2 HFO Detection

Automated HFO detection and artifact rejection resulted in 42,823 candidate events across all subjects and data. After visual validation, 11,771 HFO events remained (27.5%). Examples of candidate events that were deemed to be HFOs and false positives (artifacts) can be seen in **Figure 4**.

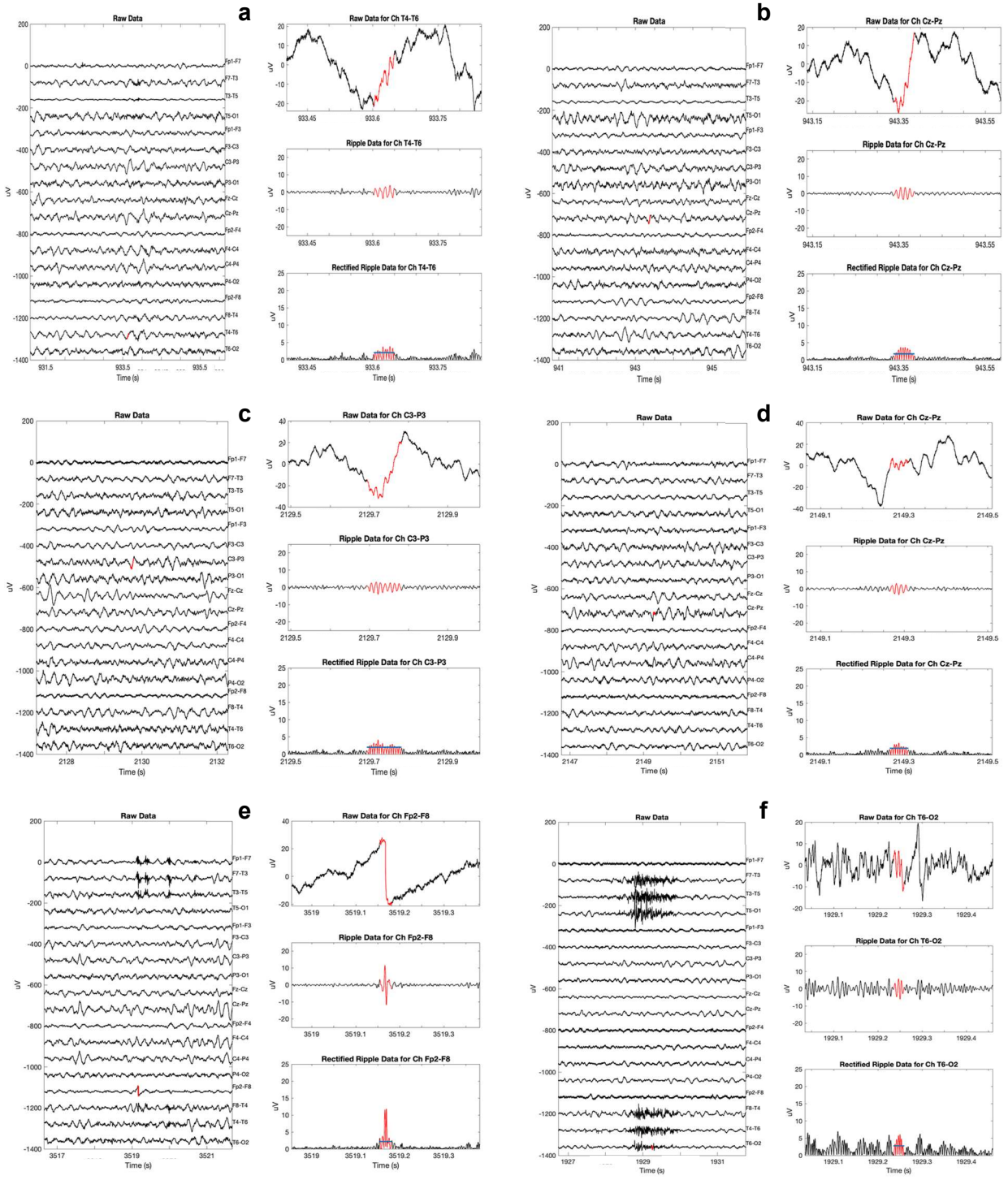

Figure 4. Examples of HFOs and artifacts recorded via scalp EEG. Examples of HFOs detected in (a) Subject 9, (b) Subject 9, (c) Subject 12, and (d) Subject 22. Detected artifacts included (e) a DC shift/ large spike with no visible oscillations from Subject 2 and (f) muscle activity in the channel and in surrounding channels from Subject 29.

3.3 Analysis

3.3.1 HFO Characteristics: Duration, RMS Amplitude, Frequency, and Global Rate

Across all subjects, the median HFO duration ranged from 28.5 to 36.0 ms, with a median duration value of 32.4 ms across all HFOs (**Figure 5a**). Median RMS amplitude for HFOs from each subject ranged from 1.73 to 3.01 μV, with a median value of 2.43 μV across all HFOs (**Figure 5b**). Median peak frequency for HFOs from each subject ranged from 93 to 105 Hz, with a median value of 99 Hz across all HFOs (**Figure 5c**). Global HFO rates ranged from 0.27 to 2.22 events/min across subjects (**Table 1**).

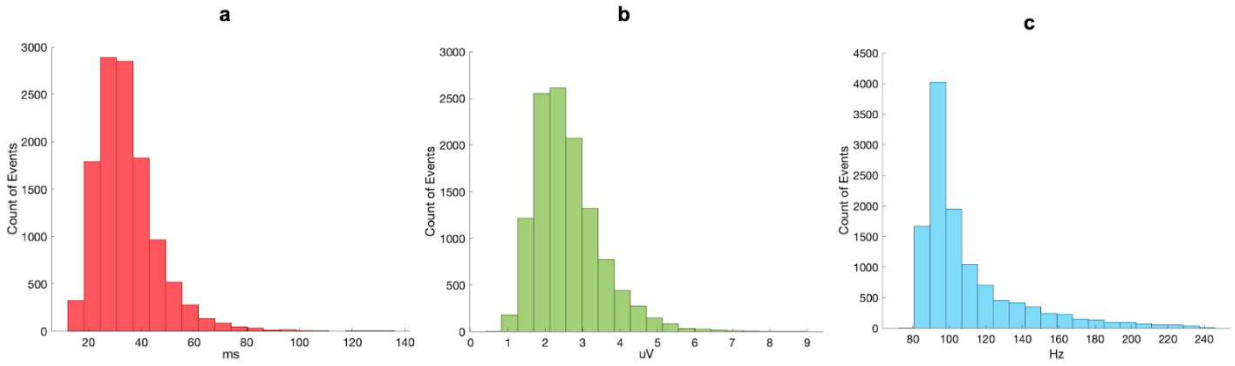

Figure 5. HFO characteristics. Histograms are shown for (a) Duration, (b) RMS amplitude, and (c) Peak frequency of all 11,771 HFO events from all 16 subjects.

3.3.2 HFO Rates are Highest in Frontal and Temporal Brain Regions

Across all subjects for all non-REM sleep, HFO rates were highest in the frontal (Fp1-F3, Fp1-F7, Fp2-F4, Fp2-F8), temporal (F7-T3, T3-T5, F8-T4, T4-T6), and prefrontal regions (F3-C3, F4-C4), followed by central regions (Fz-Cz, Cz-Pz; **Figure 6a**). Parietal and occipital regions exhibited lower HFO rates. This pattern of HFO rates was symmetric across brain

hemispheres (**Figure 6a-d**) and relatively consistent when broken down by sleep stage, although the global HFO rate decreased as sleep depth increased (**Figure 6b-d**).

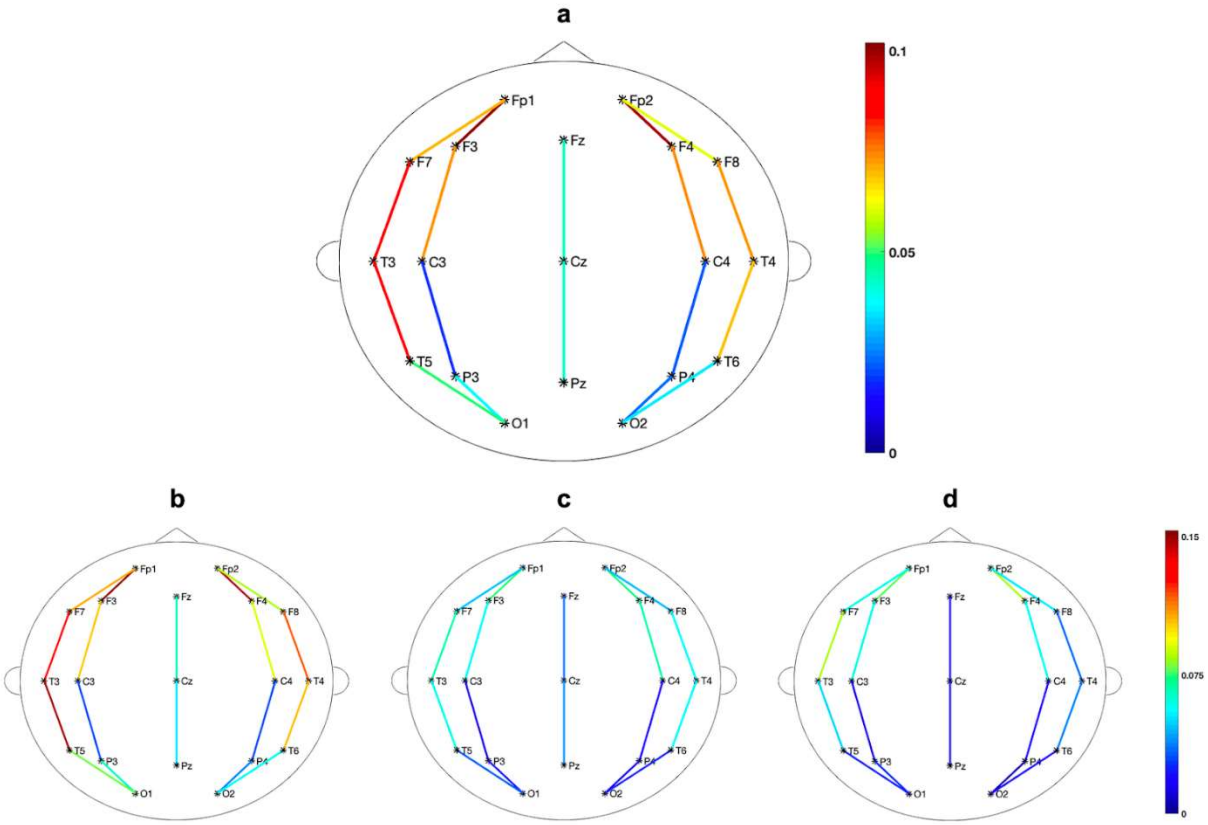

Figure 6. Spatial distribution of HFO rates across all subjects (n=16). Mean HFO rates (number per minute) are represented by the color of the line connecting each bipolar electrode pair. Results are shown for (a) all non-REM sleep, (b) N1 sleep, (c) N2 sleep, and (d) N3 sleep.

3.3.3 HFO Rate Decreases as Sleep Depth Increases

Looking at global HFO rates per sleep stage, global HFO rates were significantly different in the different stages of sleep (Friedman's ANOVA: $\chi^2 = 18.88$, $p = 7.97e\text{-}05$). Post-hoc analysis using the Wilcoxon signed-rank test showed that across subjects, global HFO rates were found to be greater in N1 sleep as compared to N2 sleep and N3 sleep (N1 vs N2: $p = 2.41e\text{-}04$, N1 vs N3: $p = 0.0017$) (**Figure 7a**). Looking at distributions of global HFO rates

per sleep stage based on rate measurements from 10-minute segments of EEG, within individual subjects, global HFO rates were found to be greater in N1 sleep as compared to N2 sleep in eight subjects, and greater in N1 sleep as compared to N3 sleep in seven subjects (Wilcoxon rank-sum test corrected using the Benjamini-Hochberg procedure with a false discovery rate of 0.05) (**Figure 7b**). The estimated HFO rate changed over time, and thus one short segment of data was not necessarily representative of all HFO activity (**Figure 7b**). The duration of time spent in each sleep stage differed within and across subjects.

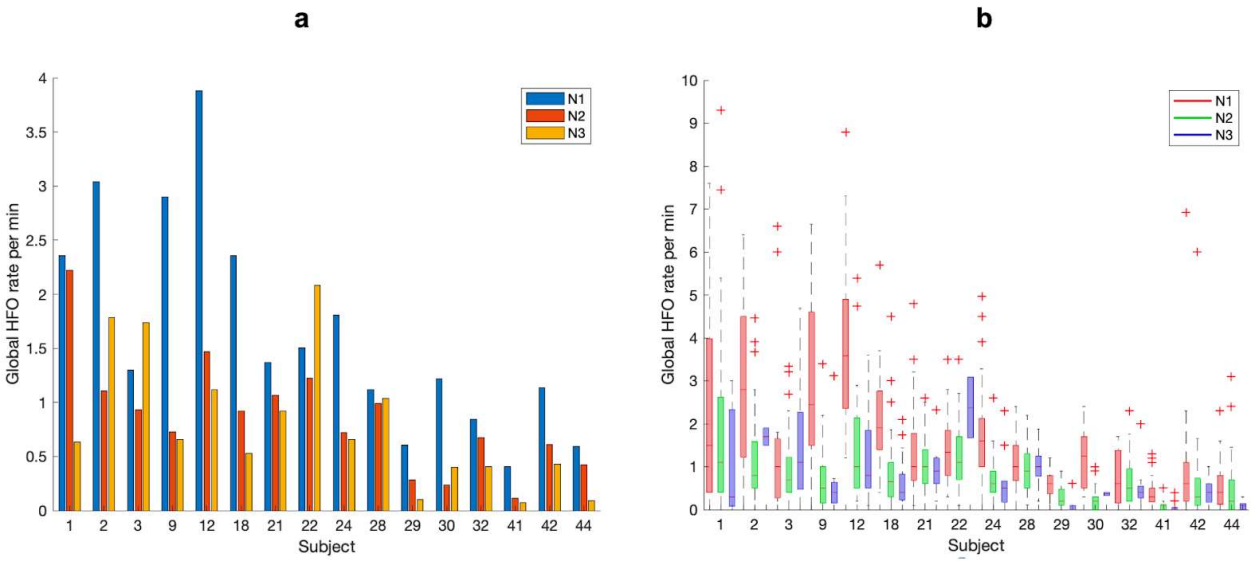

Figure 7. Global HFO rates are greater in N1 sleep than in N2 and N3 sleep. (a) Global HFO rates per sleep stage, (b) HFO rate variability per sleep stage (distributions are displayed for each sleep stage, calculated based on rate measurements from 10-minute segments of EEG; boxes represent the IQR, red '+' symbols represent individual outliers).

3.3.4 Global HFO Rate is Not Correlated with Age

We compared global HFO rate in all non-REM sleep to the subject age, but we found no relationship between these two variables (**Figure 8)**. As can be seen in **Figure 8**, we observed a wide variation in global HFO rate across the subjects.

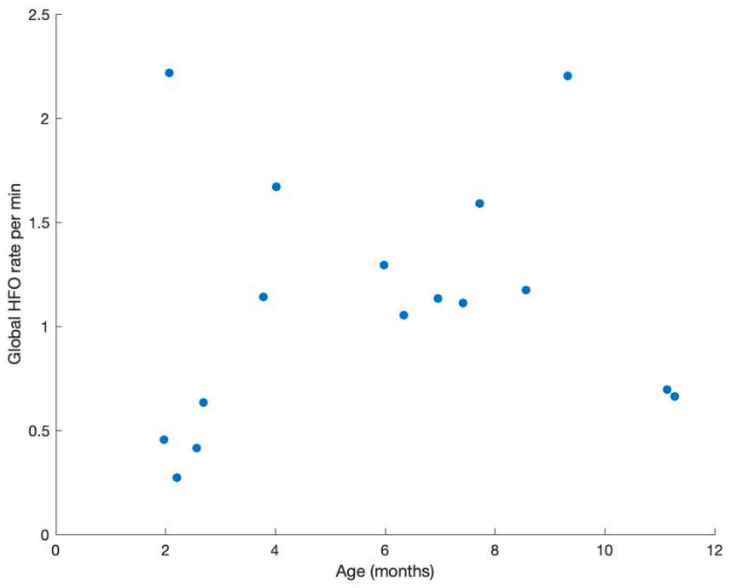

Figure 8. There is no correlation between global HFO rate and subject age.

3.3.5 Characteristics of False Positive (Artifact) Detections

We calculated the characteristics of the candidate HFOs that were rejected as artifacts based on visual analysis. This, combined with the earlier results, presents a picture of all automatically detected events and the impact of the manual validation step. Median artifact duration for each subject ranged from 29.9 to 33.4 ms, with a median duration of 31.4 ms across all artifacts. Median RMS amplitude for each subject ranged from 2.34 to 3.69 μV, with a median value of 3.06 μV across all artifacts. Median peak frequency for each subject ranged from 97 to 107 Hz, with a median value of 102 Hz across all artifacts.

Comparing artifacts to HFOs within individual subjects, duration was significantly different between the groups in eight subjects (with values for artifacts higher in four of these subjects), RMS amplitude was significantly different in all 16 subjects (with values for artifacts higher in all 16 subjects), and peak frequency was significantly different in nine

subjects (with values for artifacts higher in eight of these subjects). All Wilcoxon rank-sum tests were calculated using a significance threshold of $p < 0.0031$ based on a Bonferroni correction for 16 comparisons.

Across all subjects for all non-REM sleep, artifacts occurred most frequently in the temporal regions (F7-T3, T3-T5, F8-T4, T4-T6), followed by prefrontal regions (F3-C3, F4-C4; **Figure 9**). Parietal (C3-P3, C4-P4), parieto-occipital regions (P3-O1, P4-O2), and midline channels (Fz-Cz, Cz-Pz) had the lowest artifact rates. The low rates of artifacts in Fz-Cz (0.0219 artifacts per minute) and Cz-Pz (0.012 artifacts per minute) suggest that the majority of the automatically detected events in these channels were HFOs. Similar to HFOs, the spatial pattern of artifact rates was symmetric across brain hemispheres and was consistent across sleep stages.

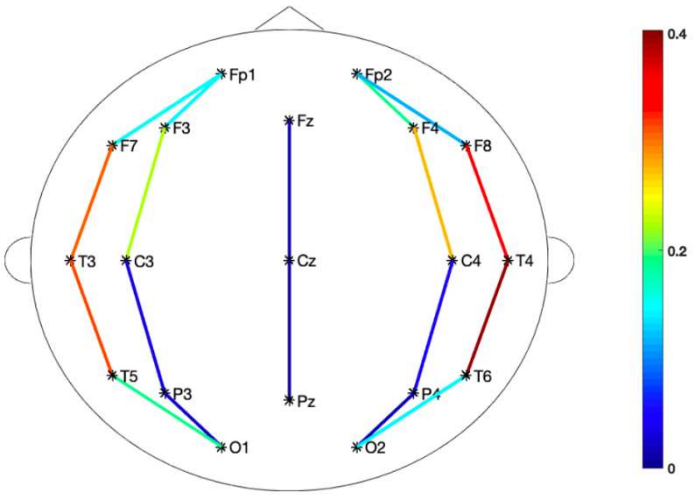

Figure 9. Spatial distribution of artifact rates (number per minute) across all subjects in all non-REM sleep.

4. DISCUSSION

Here, we report the detection of spontaneously occurring physiological ripples in the long-term scalp EEG of healthy infant subjects. Events were detected in all sixteen subjects and confirmed via visual validation. In total, 11,771 visually validated HFOs were analyzed. We found that HFO rate was highest in frontal and temporal channels, and it was highest in the lightest stage of non-REM sleep (N1). Based on 10-minute segments of EEG, the measurements of rate varied over time, with the highest variance in stage N1. We found no relationship between subject age and global HFO rate. This work represents the most comprehensive analysis of scalp physiological ripples thus far, drawing from almost 180 hours of non-REM sleep EEG. The results contribute to our understanding of the visibility and characteristics of physiological ripples on the scalp and their relationship to the stages of sleep, as well as providing a valuable baseline for studies of pathological ripples associated with epilepsy.

HFO amplitude values reported in this study are comparable to those reported in Mooij et al., 2017 and von Ellenrieder et al., 2016, while lower than those reported in Alkawadri et al., 2014 and Cimbalnik et al., 2018. However, the latter studies used intracranial recordings, thus the difference in amplitude can be expected. Peak frequency values reported in this study are comparable to those reported in Mooij et al., 2017, von Ellenrieder et al., 2016, and Alkawadri et al., 2014, while lower than those reported in Cimbalnik et al., 2018. Cimbalnik et al., 2018 studied a wider frequency range (65-600 Hz) and analyzed intracranial EEG, which likely contributed to this difference. The duration values reported in this study are lower than the 69-170 ms durations previously observed

in other studies of physiological HFOs (Mooij et al., 2017; von Ellenrieder et al., 2016; Alkawadri et al., 2014). This is possibly due to the method of detection. The automated detector we used is designed to detect the central oscillations in each event that exceed a threshold, and no windowing is used to calculate the amplitude. Thus, our reported event duration is slightly shorter than the actual event duration. In contrast, the RMS amplitude is calculated in a sliding window which leads to spreading of the amplitude estimate over time; therefore, a detector using RMS amplitude is more likely to account for smaller oscillations at the beginning or end that may visually appear to be part of the same event.

Regarding the spatial distribution of the physiological ripples, HFOs were mostly found in the prefrontal, frontal, and temporal regions, followed by central regions, with occipital regions displaying the lowest HFO rates. These results differ from the observations made in Alkawadri et al., 2014 (in which occipital channels had highest HFO rates) and Mooij et al., 2017 (in which central midline channels Cz-Pz, Fz-Cz, and Pz-O2 had the greatest number of events). Alkawadri et al., 2014 used iEEG recordings and measured HFOs in adults, all of which had epilepsy. Mooij et al., 2017 reported rates for each channel pair as the summation of HFOs across all subjects in their study, which included subjects with epilepsy. However, patients with epilepsy may exhibit both physiological and pathological events, and the spatial distributions may differ between healthy subjects and those with epilepsy. Also, the authors did not account for differences in duration of sleep analyzed per subject, so subjects with more sleep data had a greater influence on the result. Thus, direct comparison to previous works is challenging.

Artifacts must be accounted for in any analysis of scalp EEG data, and they were certainly a significant factor in our analysis. Because we found high rates of HFOs in

temporal channels (**Figure 6**), it is possible that some of the HFOs we reported were artifacts due to short bursts of muscle activity. However, we used rigorous visual validation to verify all events, which simultaneously accounted for the raw data, filtered data, and the concurrent EEG in all other channels. Any events associated with visible EEG evidence suggesting that they were of non-neural origin were rejected as artifacts. Moreover, the spatial distributions of HFO rates (**Figure 6**) and artifact rates (**Figure 9**) were different; if many artifacts were mislabeled as HFOs, we would expect the two distributions to be the same. The highest rates of HFOs were in the frontal lobe, while the highest rates of artifacts were in the temporal lobe. We also note that the central midline channels (Fz-Cz, Cz-Pz) had very low rates of artifacts (0.0219 and 0.012 HFOs/min, respectively) compared to HFO rates (0.0459 and 0.044 HFOs/min, respectively), and these channel pairs are the least impacted by muscle activity. This suggests that the majority of HFOs detected in these regions were real events and also implies that central HFOs can be reliably found through automatic detection, possibly without time-consuming visual validation.

Global HFO rates reported in this study agree with those found in Mooij et al., 2017 and von Ellenrieder et al., 2016. Across all subjects, HFO rates were found to be greater in N1 sleep as compared to N2 and N3 sleep. This result was consistent on an individual subject level in about half of the subjects. This result is partly consistent with findings in Mooij et al., 2018, as they found that ripple rates were greater in N1 and N2 sleep as compared to N3 sleep. We observed widespread temporal variability in ripple rates **(Figure 7b)**, especially in N1 sleep, which is not surprising because this stage of sleep is most transient and difficult to sleep stage. We also compared global HFO rate to subject age, but we found no clear relationship between these quantities. This observation was in

accordance with the findings in Mooij et al., 2017, where no clear trend between age and HFO rate was observed. Also, Chu et al., 2014 has reported that power in the high-frequency bands (> 65 Hz) increases from childhood to adolescence. Thus, the age range in our cohort may be too small to see any significant change with age. It is also possible that changes in HFO rate are masked by the corresponding increase in skull thickness that occurs during normal infant development.

4.1 Limitations and Future Work

Our study has several limitations, including the small number of subjects. However, to compensate for this, we analyzed large amounts of data for each subject, which increases the robustness of our results. Also, while preprocessing the data for detection, the characteristic 1/f power spectrum of EEG was not accounted for. Thus, our estimates of peak frequency may be skewed toward the lower end of the ripple band, but we note that they were consistent with reports from previous studies.

Another limitation is that we only analyzed HFOs in the ripple band (80-250 Hz), while it was previously shown that fast ripples can be detected on scalp EEG (Bernardo et al., 2018). Events in this frequency band are thought to be exclusively pathological and are typically associated with epilepsy, but it would be interesting to see if our methods could be used to detect scalp fast ripples in healthy subjects. Future work could also explore low-gamma band frequencies (40-80 Hz), as one study reported that fast oscillations occurred exclusively in the lower frequency (40-60 Hz) bands in normal infants (Kobayashi et al., 2015). Lastly, the cohort we analyzed consisted of infants less than 1 year old, which is a very limited age range and a unique period of development. With scalp EEG serving as a

viable recording modality for HFO detection in infants, future work should explore if detection is directly impacted by anatomical features such as skull thickness; if not, physiological HFOs can be studied in adult subjects, as well. By exploring physiological HFOs over a greater range of frequency bands and ages, we can better quantify the characteristics of high-frequency activity in humans and their role in human cognition. This detailed understanding will also benefit clinical studies of HFOs as a biomarker of epilepsy.

5. REFERENCES

Alkawadri, R., Gaspard, N., Goncharova, I. I., Spencer, D. D., Gerrard, J. L., Zaveri, H., Duckrow, R. B., Blumenfeld, H., & Hirsch, L. J. (2014). The spatial and signal characteristics of physiologic high frequency oscillations. *Epilepsia*, *55*(12), 1986–1995. https://doi.org/10.1111/epi.12851

Andrade-Valenca, L. P., Dubeau, F., Mari, F., Zelmann, R., & Gotman, J. (2011). Interictal scalp fast oscillations as a marker of the seizure onset zone. *Neurology*, *77*(6), 524–531. https://doi.org/10.1212/WNL.0b013e318228bee2

Axmacher, N., Elger, C. E., & Fell, J. (2008). Ripples in the medial temporal lobe are relevant for human memory consolidation. *Brain*, *131*(7), 1806–1817. https://doi.org/10.1093/brain/awn103

Bernardo, D., Nariai, H., Hussain, S. A., Sankar, R., Salamon, N., Krueger, D. A., Sahin, M., Northrup, H., Bebin, E. M., Wu, J. Y. (2018). Visual and semi-automatic non-invasive detection of interictal fast ripples: A potential biomarker of epilepsy in children with tuberous sclerosis complex. *Clinical Neurophysiology*, *129*(7), 1458–1466. https://doi.org/10.1016/j.clinph.2018.03.010

Bragin, A., Engel, J., Jr, Wilson, C. L., Fried, I., & Mathern, G. W. (1999). Hippocampal and entorhinal cortex high-frequency oscillations (100--500 Hz) in human epileptic brain and in kainic acid--treated rats with chronic seizures. *Epilepsia*, *40*(2), 127–137. https://doi.org/10.1111/j.1528-1157.1999.tb02065.x

Buzsáki, G., & Silva, F. L. (2012). High frequency oscillations in the intact brain. *Progress in Neurobiology*, *98*(3), 241–249. https://doi.org/10.1016/j.pneurobio.2012.02.004

Charupanit, K., & Lopour, B. A. (2017). A Simple Statistical Method for the Automatic Detection of Ripples in Human Intracranial EEG. *Brain Topography*, *30*(6), 724–738. https://doi.org/10.1007/s10548-017-0579-6

Charupanit, K., Nunez, M. D., Bernardo, D., Bebin, M., Krueger, D. A., Northrup, H., Sahin, M., Wu, J. Y., & Lopour, B. A. (2018). Automated Detection of High Frequency Oscillations in Human Scalp Electroencephalogram. *Proceedings of the Annual International Conference of the IEEE Engineering in Medicine and Biology Society, EMBS*, *2018-July*, pp. 3116–3119. https://doi.org/10.1109/EMBC.2018.8513033

Chrobak, J. J., & Buzsáki, G. (1996). High-frequency oscillations in the output networks of the hippocampal-entorhinal axis of the freely behaving rat. *The Journal of Neuroscience*, *16*(9), 3056–3066. https://doi.org/10.1523/JNEUROSCI.16-09-03056.1996

Chu, C. J., Leahy, J., Pathmanathan, J., Kramer, M. A., & Cash, S. S. (2014). The maturation of cortical sleep rhythms and networks over early development. *Clinical Neurophysiology*, *125*(7), 1360–1370. https://doi.org/10.1016/j.clinph.2013.11.028

Cimbalnik, J., Brinkmann, B., Kremen, V., Jurak, P., Berry, B., Gompel, J. V., Stead, M., & Worrell, G. (2018). Physiological and pathological high frequency oscillations in focal epilepsy. *Annals of Clinical and Translational Neurology*, *5*(9), 1062–1076. https://doi.org/10.1002/acn3.618

Frauscher, B., von Ellenrieder, N., Zelmann, R., Rogers, C., Nguyen, D. K., Kahane, P., Dubeau, F., & Gotman, J. (2018). High-Frequency Oscillations in the Normal Human Brain. *Annals of Neurology*, *84*(3), 374–385. https://doi.org/10.1002/ana.25304

Grenier, F., Timofeev, I., & Steriade, M. (2001). Focal synchronization of ripples (80-200 Hz) in neocortex and their neuronal correlates. *Journal of Neurophysiology*, *86*(4), 1884–1898. https://doi.org/10.1152/jn.2001.86.4.1884

Jacobs, J., Zijlmans, M., Zelmann, R., Chatillon, C. É., Hall, J., Olivier, A., Dubeau, F., & Gotman, J. (2010). High-frequency electroencephalographic oscillations correlate with outcome of epilepsy surgery. *Annals of Neurology*, *67*(2), 209–220. https://doi.org/10.1002/ana.21847

Jasper, H. H. (1958). Report of the committee on methods of clinical examination in electroencephalography. *Electroencephalography and Clinical Neurophysiology*, 10(2), 370–375. https://doi.org/10.1016/0013-4694(58)90053-1

Jones, M. S., MacDonald, K. D., Choi, B., Dudek, F. E., & Barth, D. S. (2000). Intracellular correlates of fast (>200 Hz) electrical oscillations in rat somatosensory cortex. *Journal of Neurophysiology*, *84*(3), 1505–1518. https://doi.org/10.1152/jn.2000.84.3.1505

Jrad, N., Kachenoura, A., Merlet, I., Bartolomei, F., Nica, A., Biraben, A., & Wendling, F. (2017). Automatic Detection and Classification of High-Frequency Oscillations in Depth-EEG Signals. *IEEE Transactions on Biomedical Engineering*, *64*(9), 2230–2240. https://doi.org/10.1109/TBME.2016.2633391

Kandel, A., & Buzsáki, G. (1997). Cellular-synaptic generation of sleep spindles, spike-and-wave discharges, and evoked thalamocortical responses in the neocortex of the rat. *The Journal of Neuroscience*, *17*(17), 6783–6797. https://doi.org/10.1523/JNEUROSCI.17-17-06783.1997

Kobayashi, K., Akiyama, T., Oka, M., Endoh, F., & Yoshinaga, H. (2015). A storm of fast (40-150Hz) oscillations during hypsarrhythmia in West syndrome. *Annals of Neurology*, *77*(1), 58–67. https://doi.org/10.1002/ana.24299

Kobayashi, K., Ohuchi, Y., Shibata, T., Hanaoka, Y., Akiyama, M., Oka, M., Endoh, F., & Akiyama, T. (2018). Detection of fast (40–150 Hz) oscillations from the ictal scalp EEG data of myoclonic seizures in pediatric patients. *Brain and Development*, *40*(5), 397–405. https://doi.org/10.1016/j.braindev.2018.01.004

Kobayashi, K., Yoshinaga, H., Toda, Y., Inoue, T., Oka, M., & Ohtsuka, Y. (2011). High-frequency oscillations in idiopathic partial epilepsy of childhood. *Epilepsia*, *52*(10), 1812–1819. https://doi.org/10.1111/j.1528-1167.2011.03169.x

Kramer, M. A., Ostrowski, L. M., Song, D. Y., Thorn, E. L., Stoyell, S. M., Parnes, M., Chinappen, D., Xiao, G., Eden, U. T., Staley, K. J., Stufflebeam, S. M., & Chu, C. J. (2019). Scalp recorded spike ripples predict seizure risk in childhood epilepsy better than spikes. *Brain*, *142*(5), 1296–1309. https://doi.org/10.1093/brain/awz059

Kucewicz, M. T., Cimbalnik, J., Matsumoto, J. Y., Brinkmann, B. H., Bower, M. R., Vasoli, V., Sulc, V., Meyer, F., Marsh, W. R., Stead, S. M., & Worrell, G. A. (2014). High frequency oscillations are associated with cognitive processing in human recognition memory. *Brain*, *137*(8), 2231–2244. https://doi.org/10.1093/brain/awu149

Lachaux, J. P., Axmacher, N., Mormann, F., Halgren, E., & Crone, N. E. (2012). High-frequency neural activity and human cognition: past, present and possible future of intracranial EEG research. *Progress in Neurobiology*, *98*(3), 279–301. https://doi.org/10.1016/j.pneurobio.2012.06.008

Li, Z., Park, B. K., Liu, W., Zhang, J., Reed, M. P., Rupp, J. D., Hoff, C. N., & Hu, J. (2015). A statistical skull geometry model for children 0-3 years old. *PLoS ONE*, *10*(5), e0127322. https://doi.org/10.1371/journal.pone.0127322

Liu, S., Sha, Z., Sencer, A., Aydoseli, A., Bebek, N., Abosch, A., Henry, T., Gurses, C., & Ince, N. F. (2016). Exploring the time-frequency content of high frequency oscillations for automated identification of seizure onset zone in epilepsy. *Journal of Neural Engineering*, *13*(2), 026026. https://doi.org/10.1088/1741-2560/13/2/026026

Mann, H. B., & Whitney, D. R. (1947). On a Test of Whether one of Two Random Variables is Stochastically Larger than the Other. *Annals of Mathematical Statistics*, *18*(1), 50–60. https://doi.org/10.1214/aoms/1177730491

Matsumoto, A., Brinkmann, B. H., Stead, S. M., Matsumoto, J., Kucewicz, M. T., Marsh, W. R., Meyer, F., & Worrell, G. (2013). Pathological and physiological high-frequency oscillations in focal human epilepsy. *Journal of Neurophysiology*, *110*(8), 1958–1964. https://doi.org/10.1152/jn.00341.2013

McCrimmon, C. M., Wang, P. T., Heydari, P., Nguyen, A., Shaw, S. J., Gong, H., Chui, L. A., Liu, C. Y., Nenadic, Z., & Do, A. H. (2018). Electrocorticographic Encoding of Human Gait in the Leg Primary Motor Cortex. *Cerebral Cortex*, *28*(8), 2752–2762. https://doi.org/10.1093/cercor/bhx155

Melani, F., Zelmann, R., Dubeau, F., & Gotman, J. (2013). Occurrence of scalp-fast oscillations among patients with different spiking rate and their role as epileptogenicity marker. *Epilepsy Research*, *106*(3), 345–356. https://doi.org/10.1016/j.eplepsyres.2013.06.003

Mooij, A. H., Frauscher, B., Goemans, S. A. M., Huiskamp, G. J. M., Braun, K. P. J., & Zijlmans, M. (2018). Ripples in scalp EEGs of children: Co-occurrence with sleep-specific transients and occurrence across sleep stages. *Sleep*, *41*(11), 10.1093/sleep/zsy169. https://doi.org/10.1093/sleep/zsy169

Mooij, A. H., Raijmann, R. C. M. A., Jansen, F. E., Braun, K. P. J., & Zijlmans, M. (2017). Physiological Ripples (± 100 Hz) in Spike-Free Scalp EEGs of Children With and Without Epilepsy. *Brain Topography*, *30*(6), 739–746. https://doi.org/10.1007/s10548-017-0590-y

Murin, Y., Kim, J., Parvizi, J., & Goldsmith, A. (2018). SozRank: A new approach for localizing the epileptic seizure onset zone. *PLoS Computational Biology*, *14*(1), e1005953. https://doi.org/10.1371/journal.pcbi.1005953

Nagasawa, T., Juhász, C., Rothermel, R., Hoechstetter, K., Sood, S., & Asano, E. (2012). Spontaneous and visually driven high-frequency oscillations in the occipital cortex: Intracranial recording in epileptic patients. *Human Brain Mapping*, *33*(3), 569–583. https://doi.org/10.1002/hbm.21233

Pellock, J. M., Hrachovy, R., Shinnar, S., Baram, T. Z., Bettis, D., Dlugos, D. J., Gaillard, W. D., Gibson, P. A., Holmes, G. L., Nordl, D. R., O'Dell, C., Shields, W. D., Trevathan, E., & Wheless, J. W. (2010). Infantile spasms: a U.S. consensus report. *Epilepsia*, *51*(10), 2175–2189. https://doi.org/10.1111/j.1528-1167.2010.02657.x

Plante, D. T., Goldstein, M. R., Cook, J. D., Smith, R., Riedner, B. A., Rumble, M. E., Jelenchick, L., Roth, A., Tononi, G., Benca, R. M., & Peterson, M. J. (2016). Effects of partial sleep deprivation on slow waves during non-rapid eye movement sleep: A high density EEG investigation. *Clinical Neurophysiology*, *127*(2), 1436–1444. https://doi.org/10.1016/j.clinph.2015.10.040

Polo, A., Narvaez, P., & Robles Algarín, C. (2018). Implementation of a cost-effective didactic prototype for the acquisition of biomedical signals. *Electronics (Switzerland)*, *7*(5), 77. https://doi.org/10.3390/electronics7050077

Roehri, N., Pizzo, F., Lagarde, S., Lambert, I., Nica, A., McGonigal, A., Giusiano, B., Bartolomei, F., & Bénar, C. G. (2018). High-frequency oscillations are not better biomarkers of epileptogenic tissues than spikes. *Annals of Neurology*, *83*(1), 84–97. https://doi.org/10.1002/ana.25124

Smith, M. M., Weaver, K. E., Grabowski, T. J., Rao, R. P. N., & Darvas, F. (2014). Non-invasive detection of high gamma band activity during motor imagery. *Frontiers in Human Neuroscience*, *8*, 817. https://doi.org/10.3389/fnhum.2014.00817

Sparrow, S. S., Cicchetti, D. V., Saulnier, C. A. (2016). *Vineland Adaptive Behavior Scales, Third Edition (Vineland-3)*. San Antonio, TX: Pearson.

Spring, A. M., Pittman, D. J., Aghakhani, Y., Jirsch, J., Pillay, N., Bello-Espinosa, L. E., Josephson, C., & Federico, P. (2018). Generalizability of High Frequency Oscillation Evaluations in the Ripple Band. *Frontiers in Neurology*, *9,* 510. https://doi.org/10.3389/fneur.2018.00510

St. Louis, E., Frey, L., Britton, J., Hopp, J., Korb, P., Koubeissi, M., … Pestana-Knight, E. (2016). *Electroencephalography (EEG): An Introductory Text and Atlas of Normal and Abnormal Findings in Adults, Children, and Infants*. Chicago, IL: American Epilepsy Society. https://dx.doi.org/10.5698/978-0-9979756-0-4

Staba, R. J., Wilson, C. L., Bragin, A., Fried, I., & Engel, J., Jr (2002). Quantitative analysis of high-frequency oscillations (80-500 Hz) recorded in human epileptic hippocampus and entorhinal cortex. *Journal of Neurophysiology*, *88*(4), 1743–1752. https://doi.org/10.1152/jn.2002.88.4.1743

Staba, R. J., Wilson, C. L., Bragin, A., Jhung, D., Fried, I., & Engel, J. (2004). High-frequency oscillations recorded in human medial temporal lobe during sleep. *Annals of Neurology*, *56*(1), 108–115. https://doi.org/10.1002/ana.20164

von Ellenrieder, N., Frauscher, B., Dubeau, F., & Gotman, J. (2016). Interaction with slow waves during sleep improves discrimination of physiologic and pathologic high-frequency oscillations (80-500 Hz). *Epilepsia*, *57*(6), 869–878. https://doi.org/10.1111/epi.13380

von Ellenrieder, N., Andrade-Valença, L. P., Dubeau, F., & Gotman, J. (2012). Automatic detection of fast oscillations (40-200 Hz) in scalp EEG recordings. *Clinical Neurophysiology*, *123*(4), 670–680. https://doi.org/10.1016/j.clinph.2011.07.050

von Ellenrieder, N., Beltrachini, L., Perucca, P., & Gotman, J. (2014). Size of cortical generators of epileptic interictal events and visibility on scalp EEG. *NeuroImage*, *94*, 47–54. https://doi.org/10.1016/j.neuroimage.2014.02.032

von Ellenrieder, N., Dubeau, F., Gotman, J., & Frauscher, B. (2017). Physiological and pathological high-frequency oscillations have distinct sleep-homeostatic properties. *NeuroImage. Clinical*, *14*, 566–573. https://doi.org/10.1016/j.nicl.2017.02.018

Wang, P. T., McCrimmon, C. M., King, C .E., Shaw, S. J., Millett, D. E., Gong, H., Chui, L. A., Liu, C. Y., Nenadic, Z., & Do, A. H. (2017). Characterization of electrocorticogram high-gamma signal in response to varying upper extremity movement velocity. *Brain Structure and Function, 222*(8), 3705-3748**.** https://doi.org/10.1007/s00429-017-1429-8

Wilcoxon, F. (1945). Individual Comparisons by Ranking Methods. *Biometrics Bulletin, 1*(6), 80-83. https://doi.org/10.2307/3001968

Wu, J. Y., Koh, S., Sankar, R., & Mathern, G. W. (2008). Paroxysmal fast activity: an interictal scalp EEG marker of epileptogenesis in children. *Epilepsy Research*, *82*(1), 99–106. https://doi.org/10.1016/j.eplepsyres.2008.07.010

Zelmann, R., Lina, J. M., Schulze-Bonhage, A., Gotman, J., & Jacobs, J. (2013). Scalp EEG is not a blur: It can see high frequency oscillations although their generators are small. *Brain Topography*, *27*(5), 683–704. https://doi.org/10.1007/s10548-013-0321-y

Zhang, H., Fell, J., & Axmacher, N. (2018). Electrophysiological mechanisms of human memory consolidation. *Nature Communications*, *9*(1), 4103. https://doi.org/10.1038/s41467-018-06553-y

Zijlmans, M., Jacobs, J., Zelmann, R., Dubeau, F., & Gotman, J. (2009). High-frequency oscillations mirror disease activity in patients with epilepsy. *Neurology*, *72*(11), 979–986. https://doi.org/10.1212/01.wnl.0000344402.20334.81

Zijlmans, M., Jiruska, P., Zelmann, R., Leijten, F. S., Jefferys, J. G., & Gotman, J. (2012). High-frequency oscillations as a new biomarker in epilepsy. *Annals of Neurology*, *71*(2), 169–178. https://doi.org/10.1002/ana.22548